HHS Public Access

Author manuscript

J Biomater Appl. Author manuscript; available in PMC 2020 October 01.

Published in final edited form as:

J Biomater Appl. 2019 October ; 34(4): 523–532. doi:10.1177/0885328219861614.

Polyvinyl alcohol-poly acrylic acid bilayer oral drug delivery systems: A comparison between thin films and inverse double network bilayers

Solaleh Miar, **Cynthia A Perez**, **Joo L Ong**, **Teja Guda**

University of Texas at San Antonio, San Antonio, TX, USA

Abstract

Polymer network structures in the design of bilayer hydrogels for oral drug delivery systems contribute to the mechanical stability as well as the stimulus responsive drug release. We report a strategy to improve the stability of polyelectrolyte layer interfaces in bilayer hydrogels by employing concepts from tough interpenetrating hydrogel network design. Polyvinyl alcohol as the neutral substrate and Polyacrylic acid as the pH-sensitive layer were used to prepare bilayers capable of pH-sensitive bending behavior, and inverse double network structures were compared to conventional thin film coated bilayers in this study. The morphology of the bilayers observed after exposure to stimulus revealed that the polyacrylic acid layer was fragmented in conventional thin films. The delamination of the coating also had an adverse impact on bending behavior. Additionally, bilayers with inverse double network structure had a better pH-sensitive swelling behavior which was lacking in regular thin films. Controllable, pH-specific drug release behavior was a direct benefit of using the inverse double network structure, and was demonstrated by controlled vancomycin release under different pHs chosen to simulate the physiological milieu of exposure corresponding to hydrogel passage along the gastrointestinal tract. Additionally, the inverse double networks showed improved mucoadhesive properties and mechanical stability compared to the thin film bilayers. The use of inverse double network structured hydrogels has many potential applications in improving bilayer hydrogel stability; specifically, for drug delivery systems, designing hydrogel origamis, and to prepare soft material actuators.

Keywords

Tough hydrogels; inverse double networks; thin film; oral drug delivery

Introduction

Stimulus-responsive hydrogels have been created by forming bilayers from two polymers with distinctly different responses to environmental cues. Specifically, polyelectrolyte

Corresponding author: Teja Guda, University of Texas at San Antonio, One UTSA Circle, San Anntonio, TX 78249, USA. teja.guda@utsa.edu.

Declaration of conflicting interests

The author(s) declared no potential conflicts of interest with respect to the research, authorship, and/or publication of this article.

systems have been frequently exploited as one such polymer combination.[1–3] Thin films are generally produced using conventional techniques such as photolithography,[4,5] and these bilayer hydrogels have demonstrated an ability to generate large deflections upon stimulation.[2] Depending on their molecular structure, stimulus-responsive hydrogels are able to respond to changes in the pH,[6] temperature,[7] light[8] or ionic strength[9] of the environment with a change in their volume. Through appropriate design of bilayer architecture,[10] these changes in volume may be converted into longitudinal,[11] folding,[12] rolling,[7] twisting[13] and bending movements[6] of the overall hydrogel construct. Such factors are important characteristics for biomaterials used for oral drug delivery because they can be programmed for sequential response to an acidic environment in stomach, followed by a sudden pH change in the intestine. The design of the hydrogel actuator determines the specific type of movement generated in response to the change in volume. A longitudinal movement is generated when the hydrogel is allowed to expand or contract uniformly, whereas folding or bending movement occurs when the hydrogel is locally stimulated or the actuator design is non-isotropic.[12] Various factors such as inhomogeneity in the swelling ratio[4] or the relative differences in the actuation of sections of a bilayer[9] can result in the development of anisotropic stresses in the construct curvature. Concerns such as delamination and weak attachment between the bilayer components may cause poor actuation and strategies such as interpenetrating polymer networks have been proposed to resolve such issues.[5] Furthermore, while the bio-functionality of bilayers with regards to stimulus-responsive drug release has been widely reported, there are limited degrees of quantification of their stability and bending mechanics in response to physiological stimuli.

Double network[14,15] and inverse double network (IDN) hydrogels[16,17] have recently been proposed for biomedical applications such as the regeneration of cartilage[18] and tendons,[19] or to function as artificial muscles[20] to leverage their relatively advantageous mechanical properties such as low sliding friction,[21] high extensibility and recovery,[22] and high toughness and ability to absorb shocks.[22,23] In addition to considerably improved mechanical properties, the use of polyelectrolyte hydrogels in IDNs opens up the potential for applications as smart (stimulus-responsive) drug delivery systems.[24] Generally, double network hydrogels comprise two networks wherein a brittle polyelectrolyte serves as the first network while the second network is a loosely cross-linked polymer[15] within the first network. IDN hydrogels comprised a neutral hydrogel as the primary network and a polyelectrolyte polymer as the second network.[25] The concept of using two networks has shown many benefits for stimulus responsive designs such as origami-inspired fabrications,[26,27] actuators[28] and bilayers.[10] However, interpenetration techniques such as double network and IDN systems have not been extensively explored in simple bilayers specifically. In addition, while IDN hydrogels may offer a novel approach in structures such as bilayers, the use of such stimulus responsive mechanical bilayers as drug delivery systems bears further investigation.

The current study focuses on the use of IDNs in bilayers and evaluates the impact of IDN structure on the functionality of bilayers, with the objective of developing bilayers for an oral drug delivery system. The specific polymers employed for this bilayer system are polyvinyl alcohol (PVA), a neutral hydrogel and polyacrylic acid (PAA), a pH-sensitive hydrogel. The ability to use a bilayer actuated by changes in pH to bend, and subsequently

provide greater surface area for mucosal contact is specifically investigated in this study for oral drug delivery system considerations. Additionally, in an effort to improve mechanical properties and stability of bilayer hydrogels in environments with different pH, this study also compared PAA-PVA thin films made by conventional techniques to PAA-PVA bilayers fabricated as IDNs. Delamination,[29,30] the impact of IDN hydrogels in actuation of the bilayers, and their corresponding drug release profile are characterized. Additionally, since bending deflections have previously been reported by measuring bending angle[31] or displacement distance from the zero order,[32] the bending strain of the developed bilayers are measured directly using a strain gauge in order to better quantify bilayer efficacy under stimulus.

Material and methods

Materials

In this study, acrylic acid (AA) monomers and polyvinyl alcohol (PVA) (M_w =72000 g.mol $^{-1}$, degree of hydrolysis >99%) were used to fabricate the bilayers. Ethylene glycol dimethacrylate (EGDMA) was used as the crosslinking agent, ammonium persulfate (APS) was used as the thermal initiator, and sodium disulfite (SDS) was used as the co-initiator. Vancomycin hydrochloride was used as the model antibiotic to evaluate drug release. All supplies were purchased from Sigma Aldrich (St. Louis, MO).

Sample preparation

PVA was dissolved in double distilled water (5% w/v) at 90°C for 8 h and the solution was cast into a Petri dish and maintained at 80°C for 24 h until dry. AA polymerization solution was prepared by mixing AA monomers with crosslinking agent (EGDMA), initiators (APS and SDS) and distilled water in the molar ratio of 1:0.01:0.005:0.1. To fabricate IDN bilayers, the AA polymerization solution was applied to the PVA film, followed by having the film remain in a sealed Petri dish at room temperature for 3 h to ensure diffusion of the monomer solution into the PVA film. The temperature was then elevated to 75°C for 2 h, followed by a post-polymerization step at 45°C for 24 h to complete the reaction. Thin films were made by applying AA monomer solution to the PVA film followed by immediate PAA polymerization. In all groups, the weight ratio of AA to PVA was maintained at 5:95. After the reaction, samples were washed overnight in double-distilled water and dried at room temperature. Figure 1 shows the schematic representation of the PVA, bilayers with inverse double network (IDN) and thin film (TF) bilayers prepared in this study.

Characterization

Scanning electron microscopy.—Morphological structure of the samples was observed by scanning electron microscopic (SEM) analysis (CamScan MV2300, Electron Optic Services Inc, Ottawa, ON) before and after bending experiments (detailed in Materials and Methods: Bending Actuation). Samples were prepared by first coating with silver and imaged at 20 kV. In addition, the cross sections were imaged after samples were fractured in liquid N_2 to observe the fracture surface morphology.

FTIR spectroscopic characterization.—Molecular composition of dried samples was characterized using the Fourier Transform Infrared (FTIR; Bruker Optics, Billerica, MA) in attenuated total reflection (ATR) mode. The spectrum range observed was between 1500 cm^{-1} and 2500 cm^{-1}.

Contact angle measurement.—PVA, IDN and TF membranes were evaluated using a VCA Optima contact angle (AST Products Inc., Billerica, MA) using water droplets to measure the static contact angle (Θ) for each preparation.

Stimulus responsive swelling behavior.—To compare the swelling behavior of the samples in acidic, neutral and basic environments, the dried samples were immersed at 37° in various buffer solutions (pH: 2, 7 and 9) representative of physiological milieu to determine the resultant swelling ratio. The ionic strength of all the buffers was kept constant at 0.5 M. Swollen samples were retrieved and weighed immediately after residual water was dried off the sample surface using filter paper. Equilibrium swelling ratio (equation (1))[33] was defined as the relative weight change of the wet hydrogel (W_t) as a proportion of the dried sample (W_d) weight (equation (1))

$$\text{Swelling Ratio} = \frac{wt - wd}{wd} \quad (1)$$

Mucoadhesion testing.—To evaluate the impact of bilayer structures on mucoadhesion, porcine small intestine tissue was freshly harvested and washed with PBS. Intestine specimens were used without any modifications and were affixed on polyvinyl chloride sheets. Bilayer samples (six per group) were soaked in pH 7 buffer to reach swelling equilibrium and were then cut into rectangular shapes (2 × 1 cm^2), which were affixed on polyvinyl chloride sheets. Samples and the porcine segments were then held together under 1 N load for an hour, followed by testing in lap shear mode[34] (UStretch, CellScale, Waterloo, ON).

Bending actuation.—In order to quantify deflection upon actuation by differential swelling, bending experiments were conducted by attaching a strain gauge to swollen hydrogels and measuring resultant voltage output. Samples were first immersed in a pH 2 solution to simulate the pH of the stomach, followed by attachment of the strain gauge to the swollen samples. The samples were then immediately placed in a pH 9 solution and the bending behavior was recorded using an oscilloscope (Agilent Scientific Technologies, Santa Clara, CA) for voltage readings. The area of the swollen hydrogel specimens was the same as the area of the strain gauge (1 × 0.5 cm^2), and the measurement was stopped upon reaching equilibrium voltage output (corresponding to equilibrium strain). Strain sensor BF350–3AA/1.5AA circuit was used to filter noise as well as to amplify the voltage signal. The Gauge/Sensitivity Factor and R_G of the strain gauge (Figure 2) used in this study were 2.0 and 350Ω, respectively. As detailed in equation (2),[35] where R_G is the specific resistance of the undeformed strain gauge (R_G = 350Ω) and ΔR is the change in resistance caused by the strain (ε), the strain is calculated using the voltage (V) measured by the strain gauge.

This equation is derived from the general Wheatstone bridge equation used to setup the circuit (Figure 2(a))

$$\varepsilon = \frac{\Delta R/R_G}{Gauge\ Factor} \quad (2)$$

Drug release profile.—Vancomycin was used as a model antibiotic to evaluate the drug release profile. Different quantities of antibiotic were used for each sample based on the initial sample's weight to maintain constant loading concentration. The solution containing 10 mg/mL of vancomycin was prepared and the samples were then soaked overnight at room temperature in the antibiotic solution. The volume of the antibiotic solution used did not exceed the swelling equilibrium at pH: 7 to ensure that the entire antibiotic solution was absorbed by the hydrogel samples. The release profile of the loaded vancomycin was then measured over a 10-h period using a plate reader (Synergy 2, BioTek, Winooski, VT) at 465 nm[36] in different pHs (2, 7 and 9).

Statistical analysis.—For each technique, four independent replicates were characterized and quantified. Data were statistically analyzed using one-way analysis of variance (ANOVA) across the three hydrogel designs followed by Tukey's test for *post hoc* to determine significant differences at $p < 0.05$ (SigmaPlot v14, SyStat Software Inc, San Jose, CA).

Results and discussion

The ability of oral drugs to achieve desired effects is very much dependent on their release, which in turn is dependent on the biomaterials used to deliver the drugs by leveraging the large movements generated by these hydrogels upon stimulation.[2] Depending on the molecular structure of the specific polymers used, stimuli-responsive hydrogels are able to respond to changes in environmental stimuli such as pH,[6] temperature,[7] light[8] or ionic strength[9] with a change in their volume. Further, applications such as oral drug delivery systems benefit from having a bendable structure since such changes in shape potentially provide greater exposed surface area with increased attachment to the mucus layer. In an attempt to improve the mechanical properties of these polymers in their intended environments, namely in the acidic environment of the stomach followed by a sudden change in pH in the intestinal environment, the fabrication design of bilayers was modified in the current study.

Representative surface and cross-sectional SEM micrographs of the dehydrated bilayers (Figure 3) indicated no distinct features with regards to the unmodified PVA gel whereas three distinct layers were observed in the TF and IDN designs indicating an intermediate layer, a PVA substrate and a PAA top layer. The average thickness of the PAA layer in the TF design was observed to be 33 ± 7 mm while the thickness of the PAA layer in the IDN design was observed to be 67 ± 1 μm. The intermediate layer in the TF design was also observed to be thinner compared to the IDN design, suggesting improved interpenetration of the PAA into the PVA in the IDN design. This observation is consistent with literature

reports indicating[37,38] that the immediate crosslinking of layers in TF designs achieves thinner and more distinct PAA layers compared to IDN designs. Additionally, it was also observed that the surfaces of the PAA top layers for TF designs were brittle and fragmented after exposure to both acidic and basic environments (Figure 3), suggesting the presence of a free PAA network at the surface since the pure PAA hydrogel is well known to have poor mechanical properties,[39] especially in a basic environment.[40,41] In contrast, the PVA network combined with PAA in the interfacial layer enabled the IDN design to maintain structural and morphological stability during the changes in pH.

The FTIR-ATR spectra (Figure 4) verified complete polymerization of the PAA top layer and indicated the presence of carboxylic groups (1720 cm^{-1}) in both the TF and IDN designs. The C=O band at 1711 cm^{-1} is the anhydride formation in PAA as dimers[42] in both the TF and IDN. As shown in Figure 4, there is no absorption at this band in PVA samples. A broad band in the region between 3000 cm^{-1} and 3500 cm^{-1} was also observed, indicating the presence of hydroxyl (OH) group as the most characteristic band for PVA. There is also another vibration influenced by anhydride formation at 2929 cm^{-1} known as C-H vibration.[42,43]

As shown in Figure 5, no significant difference in contact angles was observed between the PVA (control) and IDN groups, suggesting similar surface chemistry and subsequently similar hydrophilicity. Although no significant difference in contact angles was observed between the PAA and TF groups, significant differences were observed when comparing these two groups to the PVA and IDN groups. According to previous studies,[44,45] it was suggested that the presence of polar hydroxyl and carboxylic groups would increase the surface wettability, whereas the presence of crosslinking agents in the PAA may lead to the changes in the surface morphology causing the increase in the contact angle.

Figure 6 shows the swelling behavior of the PVA, IDN and TF groups after immersion in varying pH buffers over time. Non-homogeneous swelling rates were observed between the different groups tested. Figure 7 shows the swelling equilibrium of the three tested groups, with the PVA (control) group showing no significant difference in swelling ratios after immersion in different pHs. Significant differences in the swelling ratios were observed for the IDN and TF groups, with the gradual increase in swelling ratio observed in the IDN group as the pH is increased. At a pH of 9, 7 and 2, the swelling ratio for the IDN group was observed to be at 300%, 180% and 87%, respectively. With the TF group, the swelling behavior indicated sensitivity only to the basic environment (swelling ratio at pH: 9 at 211%) since no significant changes in swelling ratios were observed when the samples were immersed in buffers of pH 2 or 7. In addition, the time for the PVA hydrogel controls to achieve swelling equilibrium was 190 min and was independent of the pH. In contrast, the time for the TF and IDN groups to achieve swelling equilibrium was dependent on the pH environment. Differences between the TF and IDN groups observed were the time to achieve equilibrium, with the TF group achieving equilibrium ranging between 120 min (pH 2) to 270 min (pH 9), whereas the IDN group required a broader time range to achieve swelling equilibrium: 150 min (pH 2) to 720 min (pH 9).

PVA hydrogels have both crystalline and amorphous phases leading to outstanding mechanical properties but limiting the water uptake capacity.[46] When PAA is introduced at the surface of the IDN design, the AA forms hydrogen bonds through -COOH in addition to the physical entanglement of polymer chains, thereby generating a stable bilayer. This structure, as observed in Figure 5, would have a higher contact angle due to a denser network at the surface. It is also known that the basic environment would lead to the ionization of carboxyl groups in the PAA backbone chains. COO^- charges repel each other causing higher water uptake by the hydrogel network. As observed in this study, the swelling results suggest that the TF group retains a free PAA network on top which has limited involvement with the underlying PVA network and thereby result in increased water uptake capacity. However, the delamination observed after pH changes in the TF group (Figure 3) also suggests an overall mechanically unstable structure, which in turn impacts the effective swelling behavior of TF membranes. In contrast, the IDN group has PAA polymerized in between PVA network which not only led to increased water uptake capacity but also a stable and effective pH sensitive swelling behavior.

The mucoadhesion properties play an important role in the local availability of the drug and successive absorption into the mucosal layer.[47] Previous studies show PAA, as a carboxylic polymer, creates a significant mucoadhesion with mucus glycoprotein, while this feature can be suppressed at basic pH.[48] Since the adhesion measurement is conducted at pH: 7, the carboxylic groups in TF and IDN are unprotonated at this pH, which is higher than pKa = 4.28. Figure 8 shows the adhesion strength between the hydrogels and the intestinal mucosa. The TF group demonstrated significantly lower adhesion properties while the PVA hydrogel control showed significantly higher mucoadhesive properties among the three groups tested. This is mostly due to the higher unprotonated carboxylic groups at the surface which is lower in IDN samples due to the presence of PVA. Such differences could be also due to the mobile PAA chains in between the PVA crystalline structure that would lead to greater entanglement of chains with the mucus layer, thereby producing a mechanical adhesion mechanism.[49] The mechanical entanglement mechanism could be limited in PAA due to the use of the crosslinking agent and restriction of the PAA chain mobility.[50] Additionally, the hydroxyl groups in PVA hydrogels and the carboxylic groups in PAA are responsible for hydrogen bonding which enables an adsorption mechanism.[51] The combination of adsorption and mechanical mechanisms have been suggested to contribute to the higher mucoadhesive properties observed in PVA,[52] whereas lower adhesion strength was observed for the TF and IDN groups, which is explained by the limited PAA chain mobility at the contact surface.[47] This mechanism is also supported by the strong correlation between contact angle measurements (Figure 5) and the mucoadhesive properties, where the more hydrophilic surface demonstrate significantly higher mucoadhesion.

Vancomycin was successfully released from PVA, IDN and TF hydrogels under three different pHs (2, 7 and 9) at 37°C, over a duration of 10 h (Figure 9). A faster release was observed for the PVA group initially in the first hour, followed by a slower release rate for the remainder of the experiment. Due to the positive charge of vancomycin hydrochloride[53] and neutral nature of PVA, less drug-hydrogel charge interaction is expected to lead to passive drug release. Additionally, it was observed that 70% of the loaded vancomycin in the PVA group was released after 10 h.

In the acidic environment, the TF group released up to 55% of the loaded drug. Charge-charge interaction between PAA, vancomycin and the buffer led to an electrostatic attraction which potentially limited the release of the drug at higher rates. However, by ionization of the carboxylic acid groups of PAA in the TF in basic environments when the pH exceeds the pK_a of PAA, the ion exchange between the buffer and the hydrogel causes vancomycin to overcome the electrostatic interaction between the hydrogel and drug, which led to higher drug release. Additionally, no significant difference in the drug release was observed for the TF group when placed between pH 7 and 9. In contrast to the TF and PVA control groups, the IDN group was observed to have a relatively lower drug release of up to 67% in the basic environment and a significantly slower drug release rate in the acidic environment, suggesting a more pH-specific controlled release. As a result of the double network structure, the data suggests that the vancomycin has less charge-charge interaction with the hydrogel due to the presence of PAA in the IDN compared to the higher ratio of free PAA in the TF. However, it has also been reported that the presence of PAA in the PVA hydrogel affects drug release since PAA acts as a crosslinker at the PVA–PAA interface, which reduces polymer mesh size and effectively reduces the release rate.[54] Lower drug release rate from IDNs in acidic environment and also more controlled drug release have been suggested to be more beneficial for longer term drug release with controlled stimulus responsive release behavior.

Bending behavior of the hydrogel is considered a critical characteristic of the bilayers since no bending is observed once swelling equilibrium is achieved. Upon oral delivery, the hydrogels containing drug pass through the gastro-intestinal tract and are exposed first to an acidic environment in stomach, followed by a sudden change in pH in the intestine.[55] The bending of the bilayers in this study was studied over equilibration after a change from an acidic to a basic environment to mimic anticipated physiological milieu of exposure. No significant difference in the bending behavior was observed when the PVA control group was exposed to the different buffers (Figure 10). This insignificant bending behavior in PVA observed was anticipated since it was homogenous and uniform in structure, thus lacking the differential strain arising in bilayer designs. In contrast, significant bending behavior was observed in the TF and IDN groups, suggesting the ability of the PAA layer to induce non-homogenous swelling and thus leading to deformation of the bilayers. The greater interpenetration and binding of PAA layer into the PVA in the IDN group induced significantly higher bending strain when compared to the TF group (Figure 10). SEM micrographs in Figure 3 show the morphology of tested samples after bending measurement. The PVA control and IDN groups indicated no broken or damaged layers whereas the TF group shows broken layers which would directly impact the bending behavior. These observations suggested that interpenetration of PAA into the PVA resulted in a stronger and more effective hydrogen bonding between the two layers, thus preventing delamination of PAA after exposure to environments of different pH. This study also suggested that hydrogen bonding increased the effective stability at the interface of the IDN group while there was a lack of bonding and subsequently insufficient interfacial strength to support stimulus responsive function in the case of the TF group. Additionally, the SEM micrographs (Figure 3) also suggested that the stresses applied to the layers cause undesirable delamination of the bilayers during the stimulation, as observed in the TF group.

Conclusion

In this study, IDN and TF bilayer hydrogel fabrication was compared. It was observed that using IDN structure in bilayers improve their bending behavior by offering improved stability of layers in addition to the stimulus responsive drug release. From this study, it was concluded that the use of IDN design to deliver drugs from polyelectrolyte polymeric bilayers was more favorable stemming from both structural stability in various environments as well as greater pH sensitive control of drug release.

Funding

The author(s) received no financial support for the research, authorship, and/or publication of this article.

References

1. Ionov L Biomimetic hydrogel-based actuating systems. Adv Funct Mater 2013; 23: 4555–4570.
2. Ionov L Hydrogel-based actuators: possibilities and limitations. Mater Today 2014; 17: 494–503.
3. White EM, Yatvin J, Grubbs JB III, et al. Advances in smart materials: stimuli-responsive hydrogel thin films. J Polym Sci Polym Phys 2013; 51: 1084–1099.
4. Ionov L Soft microorigami: self-folding polymer films. Soft Matter 2011; 7: 6786–6791.
5. Erb RM, Sander JS, Grisch R, et al. Self-shaping composites with programmable bioinspired microstructures. Nat Commun 2013; 4: 1712 [PubMed: 23591879]
6. Duan J, Liang X, Zhu K, et al. Bilayer hydrogel actuators with tight interfacial adhesion fully constructed from natural polysaccharides. Soft Matter 2017; 13: 345–354. [PubMed: 27901170]
7. Kim J, Hanna JA, Hayward RC, et al. Thermally responsive rolling of thin gel strips with discrete variations in swelling. Soft Matter 2012; 8: 2375–2381.
8. Kargar-Estahbanaty A, Baghani M and Arbabi N. Developing an analytical solution for photo-sensitive hydrogel bilayers. J Intell Mater Sys Struct 2018; 29: 1953–1963.
9. Bassik N, Abebe BT, Laflin KE, et al. Photolithographically patterned smart hydrogel based bilayer actuators. Polymer 2010; 51: 6093–6098.
10. Shim TS, Kim SH, Heo CJ, et al. Controlled origami folding of hydrogel bilayers with sustained reversibility for robust microcarriers. Angew Chem 2012; 124: 1449–1452.
11. Peng X and Wang H. Shape changing hydrogels and their applications as soft actuators. J Polym Sci Polym Phys 2018; 56: 1314–1324.
12. Leong TG, Zarafshar AM and Gracias DH. Three-dimensional fabrication at small size scales. Small 2010; 6: 792–806. [PubMed: 20349446]
13. Bakarich SE, Pidcock GC, Balding P, et al. Recovery from applied strain in interpenetrating polymer network hydrogels with ionic and covalent cross-links. Soft Matter 2012; 8: 9985–9988.
14. Gong JP, Katsuyama Y, Kurokawa T, et al. Double-network hydrogels with extremely high mechanical strength. Adv Mater 2003; 15: 1155–1158.
15. Gong JP. Why are double network hydrogels so tough? Soft Matter 2010; 6: 2583–2590.
16. Myung D, Waters D, Wiseman M, et al. Progress in the development of interpenetrating polymer network hydrogels. Polym Adv Technol 2008; 19: 647–657. [PubMed: 19763189]
17. Haque MA, Kurokawa T and Gong JP. Super tough double network hydrogels and their application as biomaterials. Polymer 2012; 53: 1805–1822.
18. Arnold MP, Daniels AU, Ronken S, et al. Acrylamide polymer double-network hydrogels: Candidate cartilage repair materials with cartilage-like dynamic stiffness and attractive surgery-related attachment mechanics. Cartilage. 2011; 2: 374–383. [PubMed: 26069595]
19. Yuk H, Zhang T, Lin S, et al. Tough bonding of hydrogels to diverse non-porous surfaces. Nature Mater 2016; 15: 190 [PubMed: 26552058]

20. Liang S, Yu QM, Yin H, et al. Ultrathin tough double network hydrogels showing adjustable muscle-like isometric force generation triggered by solvent. Chem Commun 2009; 7518–7520.
21. Lin H-R, Ling M-H and Lin Y-J. High strength and low friction of a PAA-alginate-silica hydrogel as potential material for artificial soft tissues. J Biomater Sci Polym Ed 2009; 20: 637–652. [PubMed: 19323881]
22. Sun J-Y, Zhao X, Illeperuma WR, et al. Highly stretchable and tough hydrogels. Nature 2012; 489: 133 [PubMed: 22955625]
23. Illeperuma WR, Sun J-Y, Suo Z, et al. Fiber-reinforced tough hydrogels. Extr Mech Lett 2014; 1: 90–96.
24. Liu J, Pang Y, Zhang S, et al. Triggerable tough hydrogels for gastric resident dosage forms. Nat Commun 2017; 8: 124 [PubMed: 28743858]
25. Liu Y, He W, Zhang Z, et al. Recent developments in tough hydrogels for biomedical applications. Gels 2018; 4: 46
26. Jamal M, Kadam SS, Xiao R, et al. Bio-origami hydrogel scaffolds composed of photocrosslinked PEG bilayers. Adv Healthcare Mater 2013; 2: 1142–1150.
27. Na JH, Evans AA, Bae J, et al. Programming reversibly self-folding origami with micropatterned photo-crosslinkable polymer trilayers. Adv Mater 2015; 27: 79–85. [PubMed: 25362863]
28. Gracias DH. Stimuli responsive self-folding using thin polymer films. Curr Opin Chem Eng 2013; 2: 112–119.
29. Yang S, Khare K and Lin PC. Harnessing surface wrinkle patterns in soft matter. Adv Funct Mater 2010; 20: 2550–2564.
30. Zhou Z, Li Y, Wong W, et al. Transition of surface–interface creasing in bilayer hydrogels. Soft Matter 2017; 13: 6011–6020. [PubMed: 28782771]
31. Shang J, Shao Z and Chen X. Chitosan-based electroactive hydrogel. Polymer 2008; 49: 5520–5525.
32. Li S, Vogt DM, Rus D, et al. Fluid-driven origami-inspired artificial muscles. Proc Natl Acad Sci USA 2017; 114: 13132–13137 [PubMed: 29180416]
33. Peppas NA and Merrill EW. Crosslinked poly (vinyl alcohol) hydrogels as swollen elastic networks. J Appl Polym Sci 1977; 21: 1763–1770.
34. Murphy JL, Vollenweider L, Xu F, et al. Adhesive performance of biomimetic adhesive-coated biologic scaffolds. Biomacromolecules 2010; 11: 2976–2984. [PubMed: 20919699]
35. Hoffmann K Applying the wheatstone bridge circuit. Germany: HBM, 1974.
36. Abed SS and Hussein OT. Spectrophotometric determination of vancomycin hydrochloride (batch and flow-injection) using O-nitroaniline as diazotized chromogenic reagent. Iraqi J Sci 2015; 56: 3025–3035.
37. Feng Y, Smith CS and Burkett SL. Process for patterning features in poly (acrylic acid) for microelectronic applications. J Micromech Microeng 2017; 27: 055007
38. Nguyen N-T and Liu J-H. Fabrication and characterization of poly (vinyl alcohol)/chitosan hydrogel thin films via UV irradiation. Eur Polym J 2013; 49: 4201–4211.
39. Jeong J, Baik J, An S, et al. Development and characterization of cross-linked poly (acrylic acid) hydrogel containing drug by radiation-based techniques. Preprints 2018 DOI: 10.20944/preprints201801.0028.v1.
40. Anseth KS, Bowman CN and Brannon-Peppas L. Mechanical properties of hydrogels and their experimental determination. Biomaterials 1996; 17: 1647–1657. [PubMed: 8866026]
41. Kim D and Park K. Swelling and mechanical properties of superporous hydrogels of poly (acrylamide-co-acrylic acid)/polyethylenimine interpenetrating polymer networks. Polymer 2004; 45: 189–196.
42. Arndt KF, Richter A, Ludwig S, et al. Poly (vinyl alcohol)/poly (acrylic acid) hydrogels: FT-IR spectroscopic characterization of crosslinking reaction and work at transition point. Acta Polymerica 1999; 50: 383–390.
43. Socrates G Infrared characteristic group frequencies, tables and charts. J Am Chem Soc 1995; 117: 1671–

44. Wahid MNA, Abd Razak SI, Abdul Kadir MR, et al. Influence of citric acid on the physical and biomineralization ability of freeze/thaw poly (vinyl alcohol) hydrogel. J Biomater Appl 2018; 33: 94–102. [PubMed: 29716417]
45. Yadav V, Harkin AV, Robertson ML, et al. Hysteretic memory in pH-response of water contact angle on poly (acrylic acid) brushes. Soft Matter 2016; 12: 3589–3599. [PubMed: 26979270]
46. Hassan CM and Peppas NA. Structure and applications of poly (vinyl alcohol) hydrogels produced by conventional crosslinking or by freezing/thawing methods In: Biopolymers PVA hydrogels, anionic polymerization nanocomposites. Berlin, Heidelberg: Springer, 2000, vol 153, pp. 37–65.
47. Park H and Robinson JR. Mechanisms of mucoadhesion of poly (acrylic acid) hydrogels. Pharm Res 1987; 4: 457–464. [PubMed: 3508557]
48. Patel MM, Smart JD, Nevell TG, et al. Mucin/poly (acrylic acid) interactions: a spectroscopic investigation of mucoadhesion. Biomacromolecules 2003; 4: 1184–1190. [PubMed: 12959582]
49. Peppas NA and Sahlin JJ. Hydrogels as mucoadhesive and bioadhesive materials: a review. Biomaterials 1996; 17: 1553–1561. [PubMed: 8842358]
50. Alexander A, Sharma S and Khan MJ. Theories and factors affecting mucoadhesive drug delivery systems: a review. Int J Res Ayurveda Pharm 2011; 2: 1155–1161.
51. Kinloch A. Adhesion and adhesives: science and technology. New York: Chapman and Hall, 1987.
52. Cook SL, Bull SP, Methven L, et al. Mucoadhesion: a food perspective. Food Hydrocoll 2017; 72: 281–296.
53. Gustafson CT, Boakye-Agyeman F, Brinkman CL, et al. Controlled delivery of vancomycin via charged hydrogels. PloS One 2016; 11: e0146401 [PubMed: 26760034]
54. Byun H, Hong B, Nam SY, et al. Swelling behavior and drug release of poly (vinyl alcohol) hydrogel cross-linked with poly (acrylic acid). Macromol Res 2008; 16: 189–193.
55. Fallingborg J Intraluminal pH of the human gastrointestinal tract. Danish Med Bull 1999; 46: 183–196. [PubMed: 10421978]

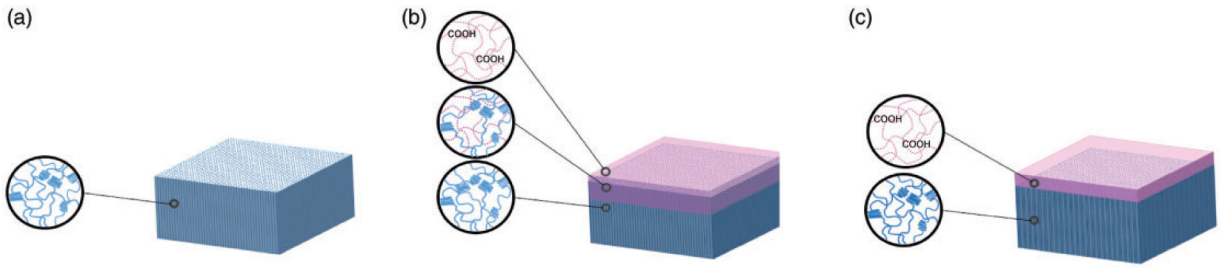

Figure 1.

Schematic image of (a) PVA, (b) IDN and (c) TF membranes. The PVA membrane comprises pure PVA chains with physical crosslinks, which causes crystalline regions in the membrane. TF has a PAA coating layer with minimized interaction with the PVA layer while the IDN has an intermediate layer which indicates the polymerization of PAA within the PVA layer. PVA: polyvinyl alcohol; IDN: inverse double network; TF: thin film; PAA: polyacrylic acid.

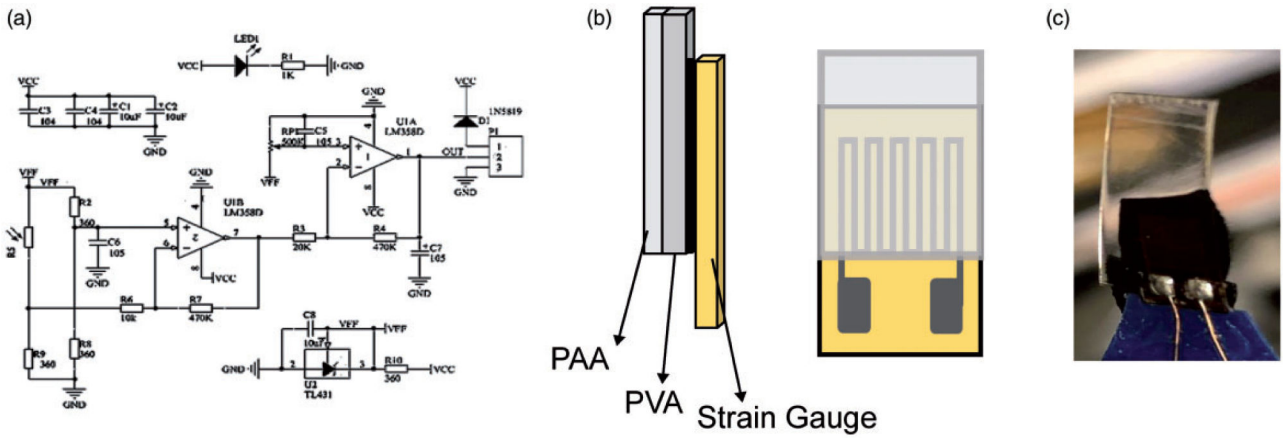

Figure 2.

(a) Strain gauge circuit diagram: schematic of circuit used to filter noise and amplify voltage signal form the strain gauge. (b) Schematic image of membranes attached to the strain gauge from the substrate side. (c) The image of membranes attached to the strain gauge by carbon tape as prepared.

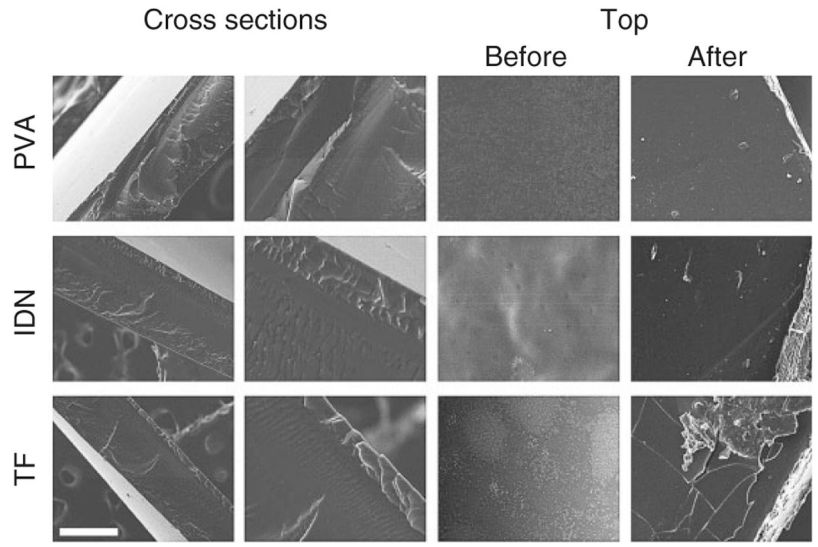

Figure 3.

SEM images of surface and cross section of PVA, IDN and TF. Different layers of PAA interpenetration into PVA were observed in both IDN and TF. The average thickness of the thin film was 33 ± 7 mm and IDN thickness was 67 ± 1 μm. Samples were also imaged after being exposed to acidic and basic environments. The images show broken pieces of the PAA layer on the TF surface while IDN showed no delamination. Imaging was conducted at 20 kV (Scale bar is 100 mm). PVA: polyvinyl alcohol; IDN: inverse double network; TF: thin film; PAA: polyacrylic acid.

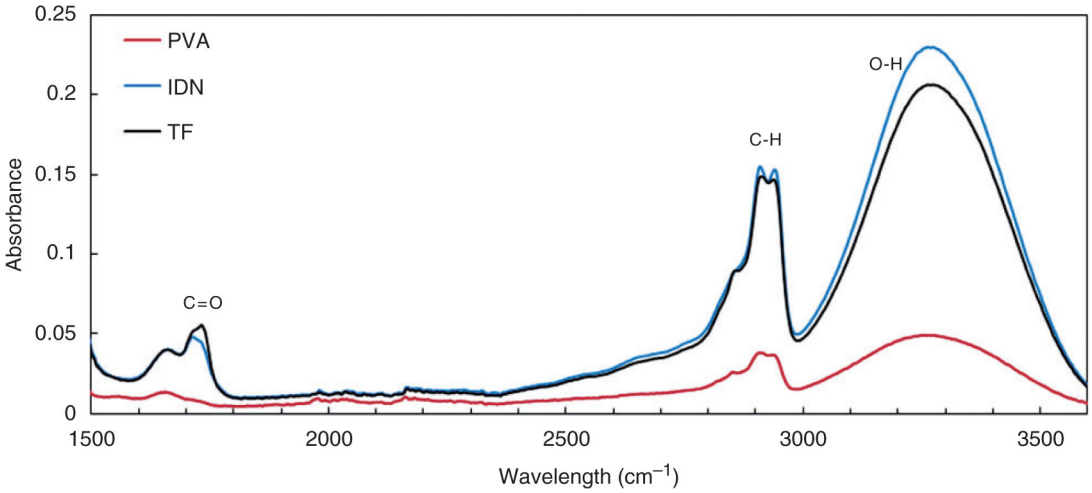

Figure 4.

ATR-FTIR results of PVA, IDN and TF membranes. The presence of hydroxyl and carboxyl groups were observed at 3000 to 3500 cm^{-1} and 1720 cm^{-1}, respectively. This indicates PAA polymerization in both the IDN and TF samples. ATR-FTIR: Fourier Transform Infrared–attenuated total reflection; PVA: polyvinyl alcohol; IDN: inverse double network; TF: thin film; PAA: polyacrylic acid.

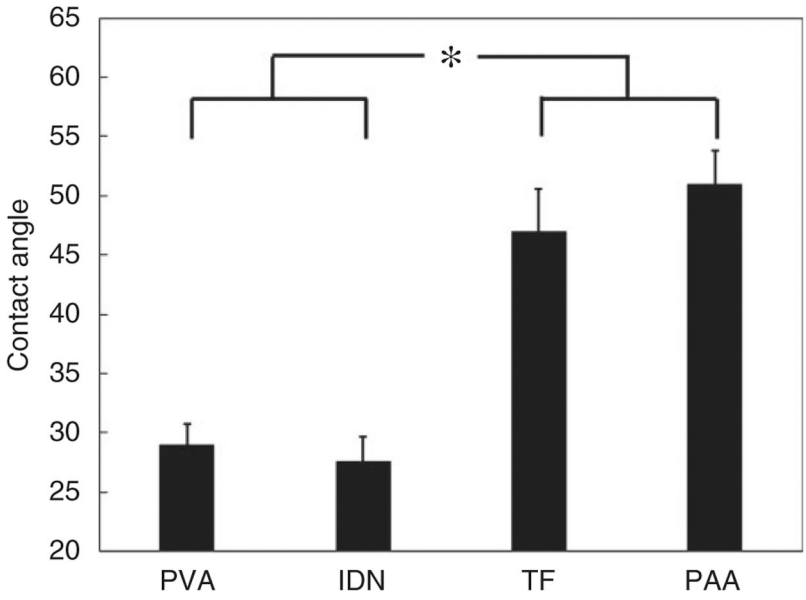

Figure 5.

Contact angle measurement of PVA, IDN, TF and IDN membranes to compare surface hydrophilicity. Contact angle results for TF and PAA were significantly different (*, $p < 0.05$) compared to IDN and PVA. PAA and TF showed similar contact angle (47 and 50°, respectively) while PVA and IDN reveal similar hydrophilicity (contact angles of 29 and 27°, respectively).

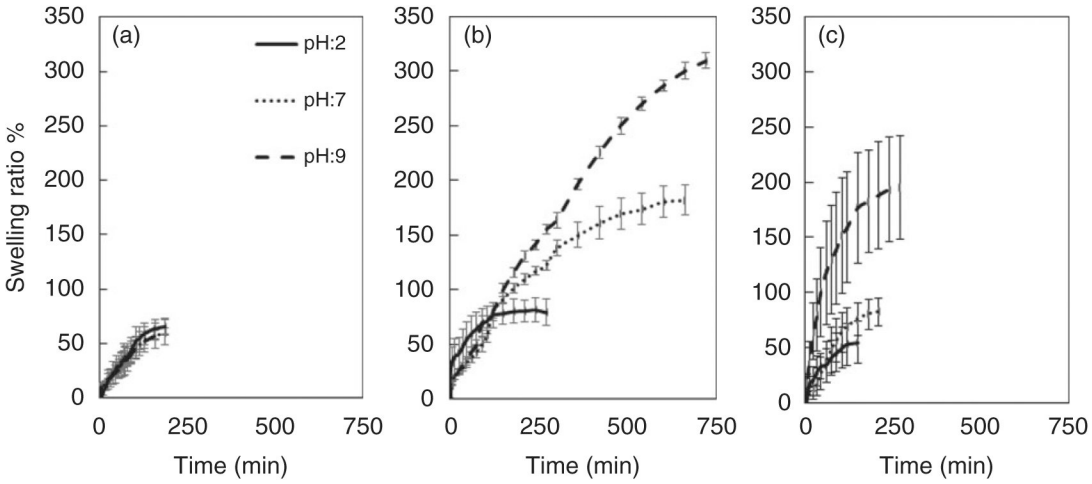

Figure 6.

Swelling behavior of (a) PVA, (b) IDN and (c) TF membranes in buffers of varying pH (2, 7 and 9) over time. PVA: polyvinyl alcohol; IDN: inverse double network; TF: thin film.

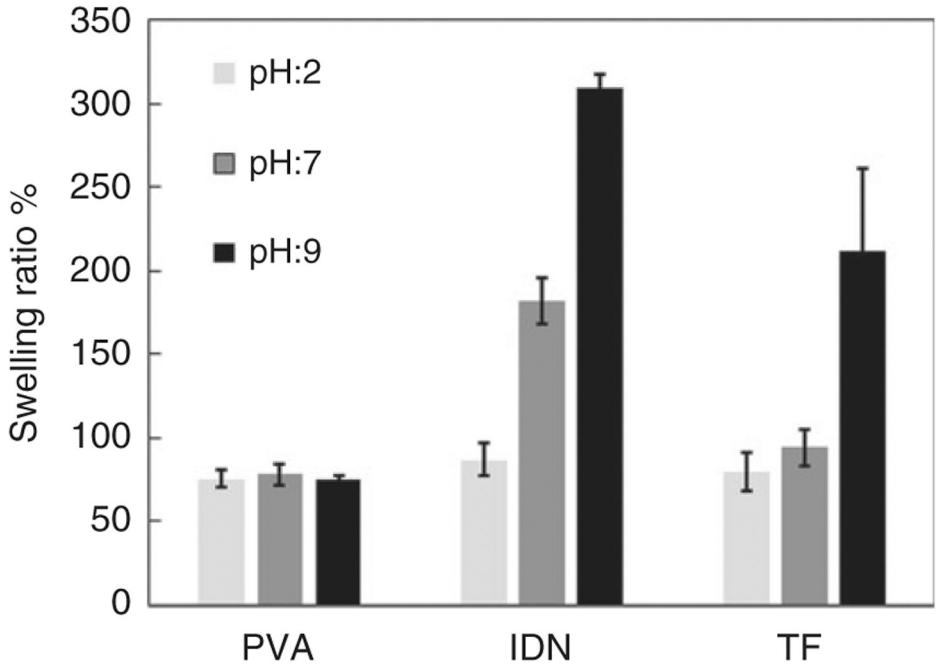

Figure 7.
Swelling equilibrium of PVA, IDN and TF in buffers of pH 2, 7 and 9 indicating maximum possible water uptake per sample. PVA: polyvinyl alcohol; IDN: inverse double network; TF: thin film.

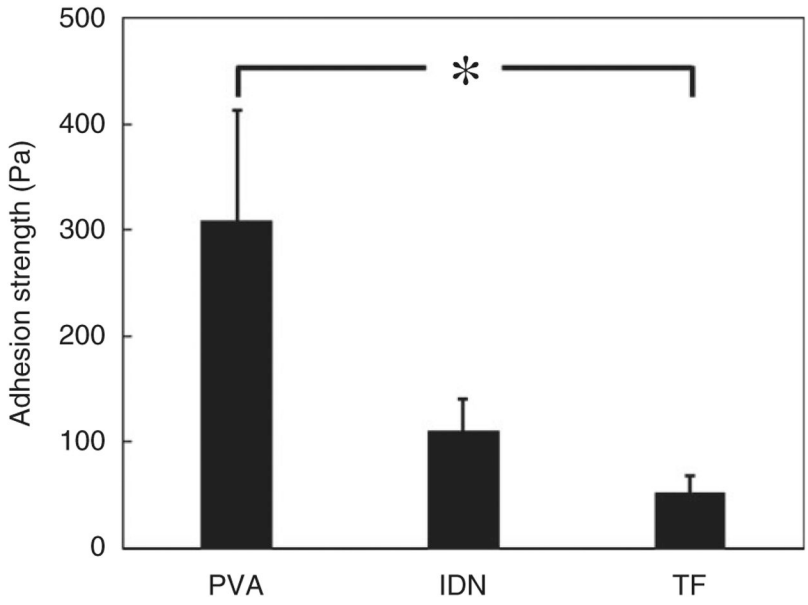

Figure 8.

Mucoadhesion testing of PVA, IDN and TF on porcine small intestinal mucosa indicating detachment force required in PBS. Samples reached swelling equilibrium and were tested using a single lap shear configuration after being adhered under 1 N load. PVA: polyvinyl alcohol; IDN: inverse double network; TF: thin film.

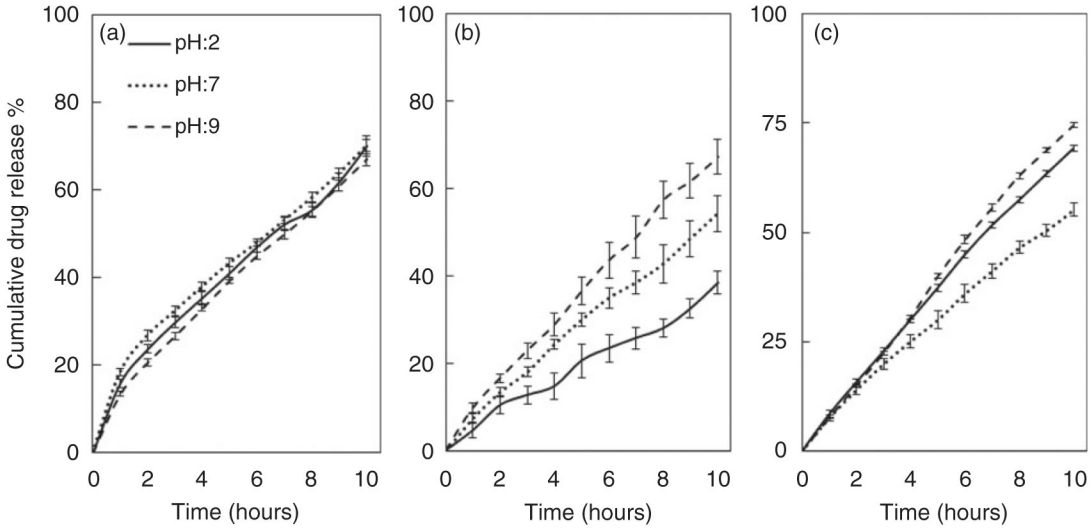

Figure 9.

Drug release profile of (a) PVA, (b) IDN and (c) TF over time. Cumulative drug release of vancomycin was quantified every hour for each group in three buffers with varying pH (2, 7 and 9). PVA: polyvinyl alcohol; IDN: inverse double network; TF: thin film.

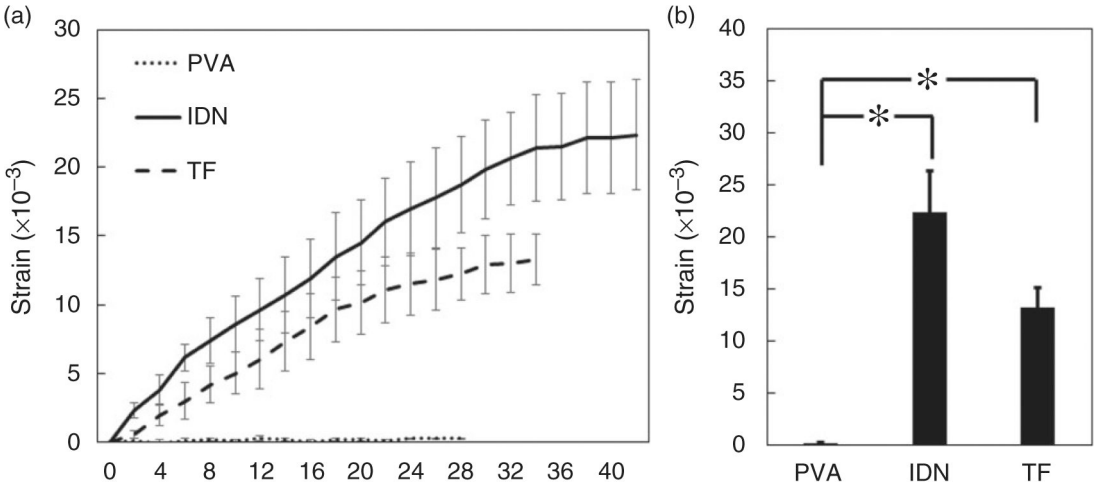

Figure 10.

(a) Bending of PVA, IDN and TF after transfer from a buffer of pH 2 to pH 9 over time. (b) The bending equilibrium of tested membranes. Changes in strain were reported to monitor bending behavior and measured at two-minute intervals. Bending equilibrium of IDN and TF were significantly different from PVA bending strain (*, $p < 0.05$). PVA: polyvinyl alcohol; IDN: inverse double network; TF: thin film.